Supplementary materials for Human-induced climate change intensifies spatially compounding fire weather extremes across European countries

Emilie Gauthier[1,*] and Emanuele Bevacqua[1]

1. Department of Compound Environmental Risks, Helmholtz Centre for Environmental Research – UFZ, Leipzig, Germany.

[*] Corresponding author: Emilie Gauthier (emilie.gauthier@ufz.de)

CMIP6 model	Native Latitude x Longitude	Ensemble members
ACCESS-CM2	1.25° × 1.88°	r1i1p1f1, r2i1p1f1, r3i1p1f1
ACCESS-ESM1-5	1.25° × 1.88°	r1i1p1f1, r2i1p1f1, r3i1p1f1, r4i1p1f1, r5i1p1f1, r6i1p1f1, r7i1p1f1, r8i1p1f1, r9i1p1f1, r10i1p1f1, r11i1p1f1, r12i1p1f1, r13i1p1f1, r14i1p1f1, r15i1p1f1, r16i1p1f1, r17i1p1f1, r18i1p1f1, r19i1p1f1, r20i1p1f1, r21i1p1f1, r22i1p1f1, r23i1p1f1, r24i1p1f1, r25i1p1f1, r26i1p1f1, r27i1p1f1, r28i1p1f1, r29i1p1f1, r30i1p1f1, r31i1p1f1, r32i1p1f1, r33i1p1f1, r34i1p1f1, r35i1p1f1, r36i1p1f1, r37i1p1f1, r38i1p1f1, r39i1p1f1, r40i1p1f1
CMCC-ESM2	0.94° × 1.25°	r1i1p1f1
CanESM5	2.79° × 2.81°	r1i1p1f1, r1i1p2f1, r2i1p1f1, r2i1p2f1, r3i1p1f1, r3i1p2f1, r4i1p1f1, r4i1p2f1, r5i1p1f1, r5i1p2f1, r6i1p1f1, r6i1p2f1, r7i1p1f1, r7i1p2f1, r8i1p1f1, r8i1p2f1, r9i1p1f1, r9i1p2f1, r10i1p1f1, r10i1p2f1, r11i1p1f1, r11i1p2f1, r12i1p1f1, r12i1p2f1, r13i1p1f1, r13i1p2f1, r14i1p1f1, r14i1p2f1, r15i1p1f1, r15i1p2f1, r16i1p1f1, r16i1p2f1, r17i1p1f1, r17i1p2f1, r18i1p1f1, r18i1p2f1, r19i1p1f1, r19i1p2f1, r20i1p1f1, r20i1p2f1, r21i1p1f1, r21i1p2f1, r22i1p1f1, r22i1p2f1, r23i1p1f1, r23i1p2f1, r24i1p1f1, r24i1p2f1, r25i1p1f1, r25i1p2f1
EC-Earth3	0.70° × 0.70°	r1i1p1f1, r4i1p1f1

EC-Earth3-Veg	0.70° × 0.70°	r2i1p1f1, r3i1p1f1, r4i1p1f1, r12i1p1f1
FGOALS-g3	2.09° × 2.00°	r1i1p1f1, r3i1p1f1, r4i1p1f1, r5i1p1f1
INM-CM4-8	1.50° × 2.00°	r1i1p1f1
INM-CM5-0	1.50° × 2.00°	r1i1p1f1, r2i1p1f1, r3i1p1f1, r4i1p1f1, r5i1p1f1
IPSL-CM6A-LR	1.27° × 2.50°	r1i1p1f1, r2i1p1f1, r3i1p1f1, r4i1p1f1, r5i1p1f1, r6i1p1f1, r7i1p1f1, r8i1p1f1, r9i1p1f1, r10i1p1f1, r14i1p1f1
KACE-1-0-G	1.25° × 1.88°	r1i1p1f1, r2i1p1f1, r3i1p1f1
MIROC-ES2L	2.79° × 2.81°	r1i1p1f2, r2i1p1f2, r3i1p1f2, r4i1p1f2, r5i1p1f2, r6i1p1f2, r7i1p1f2, r8i1p1f2, r9i1p1f2, r10i1p1f2
MIROC6	1.40° × 1.41°	r1i1p1f1
MPI-ESM-1-2-HAM	1.87° × 1.88°	r1i1p1f1, r2i1p1f1, r3i1p1f1
MPI-ES1-2-HR	0.94° × 0.94°	r1i1p1f1, r2i1p1f1, r3i1p1f1, r4i1p1f1, r5i1p1f1, r6i1p1f1, r7i1p1f1, r8i1p1f1, r9i1p1f1, r10i1p1f1
MPI-ESM1-2-LR	1.87° × 1.88°	r1i1p1f1, r2i1p1f1, r3i1p1f1, r4i1p1f1, r5i1p1f1, r6i1p1f1, r7i1p1f1, r8i1p1f1, r9i1p1f1, r10i1p1f1
MRI-ESM2-0	1.12° × 1.12°	r1i1p1f1, r2i1p1f1, r3i1p1f1, r4i1p1f1, r5i1p1f1

Supplementary Table 1. ***CMIP6 climate models.*** *List of the CMIP6 climate models used in the analysis, along with their native grid resolutions and the ensemble members included in this study.*

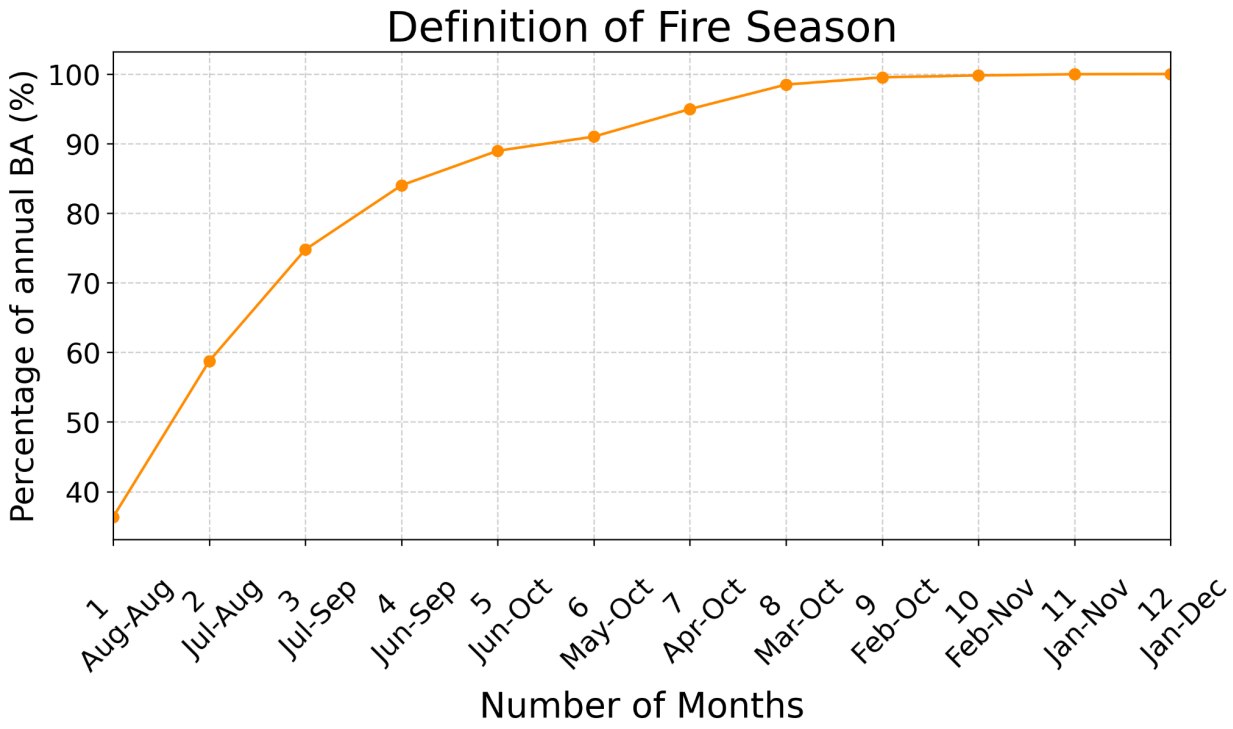

Supplementary Fig. 1. ***Definition of the fire season over Europe.*** *To define the European fire season, for N from 1 to 12 (x-axis), we evaluate all possible windows of N consecutive months and select the one encompassing the largest proportion (%) of accumulated annual burned area (BA) over 2001-2015. The x-axis states the selected window for each N, and the y-axis indicates the corresponding proportion (%) of accumulated annual burned area. The fire season is defined as the shortest window capturing ≥90% of the accumulated annual burned area, which results in selecting the 6-months period May–October.*

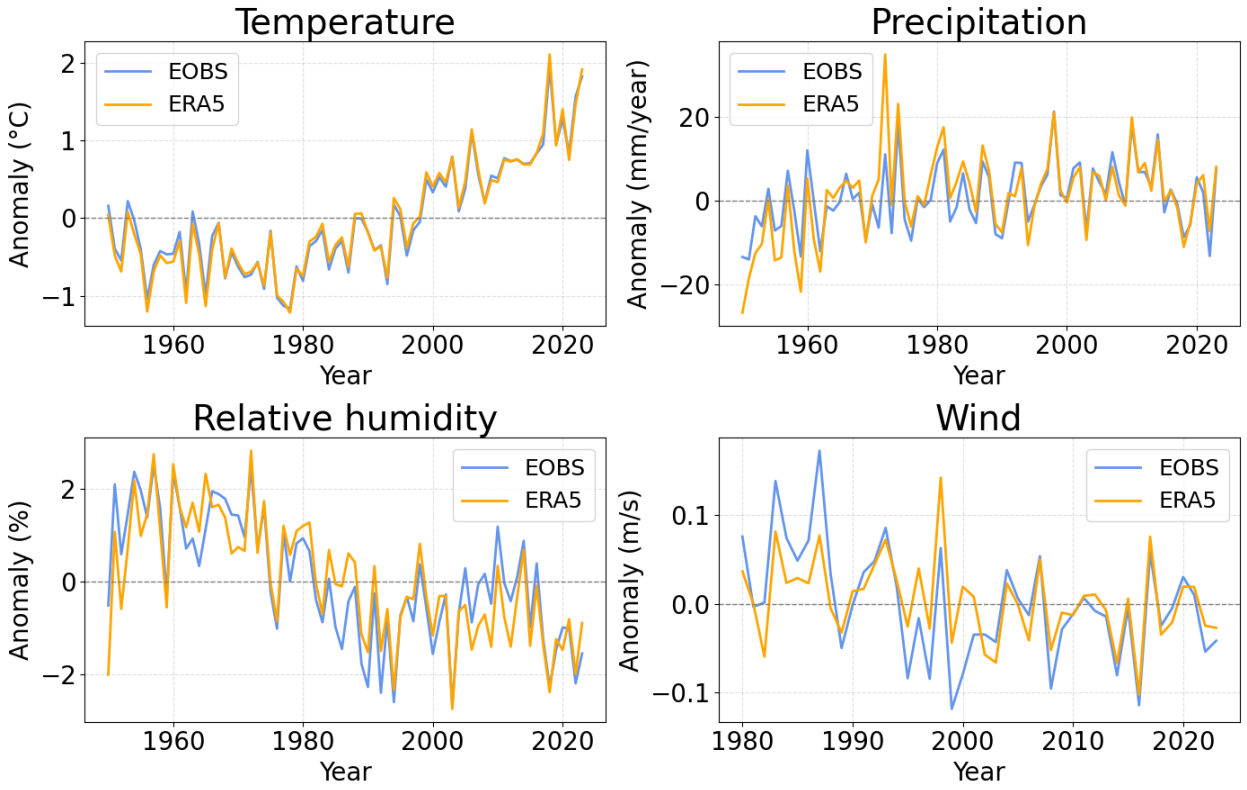

Supplementary Fig. 2. ***Comparison of EOBS and ERA5 anomalies over Europe during the fire season (May–October).*** *Annual anomalies averaged over Europe during the fire season for:* ***a*** *Temperature,* ***b*** *Precipitation,* ***c*** *Relative humidity, and* ***d*** *Wind speed. Blue curves represent results for EOBS, and orange curves for ERA5. Anomalies are computed relative to the 1950-2024 means for Temperature, Precipitation and Relative humidity; and relative to the 1980-2024 mean for Wind speed following availability of the data.*

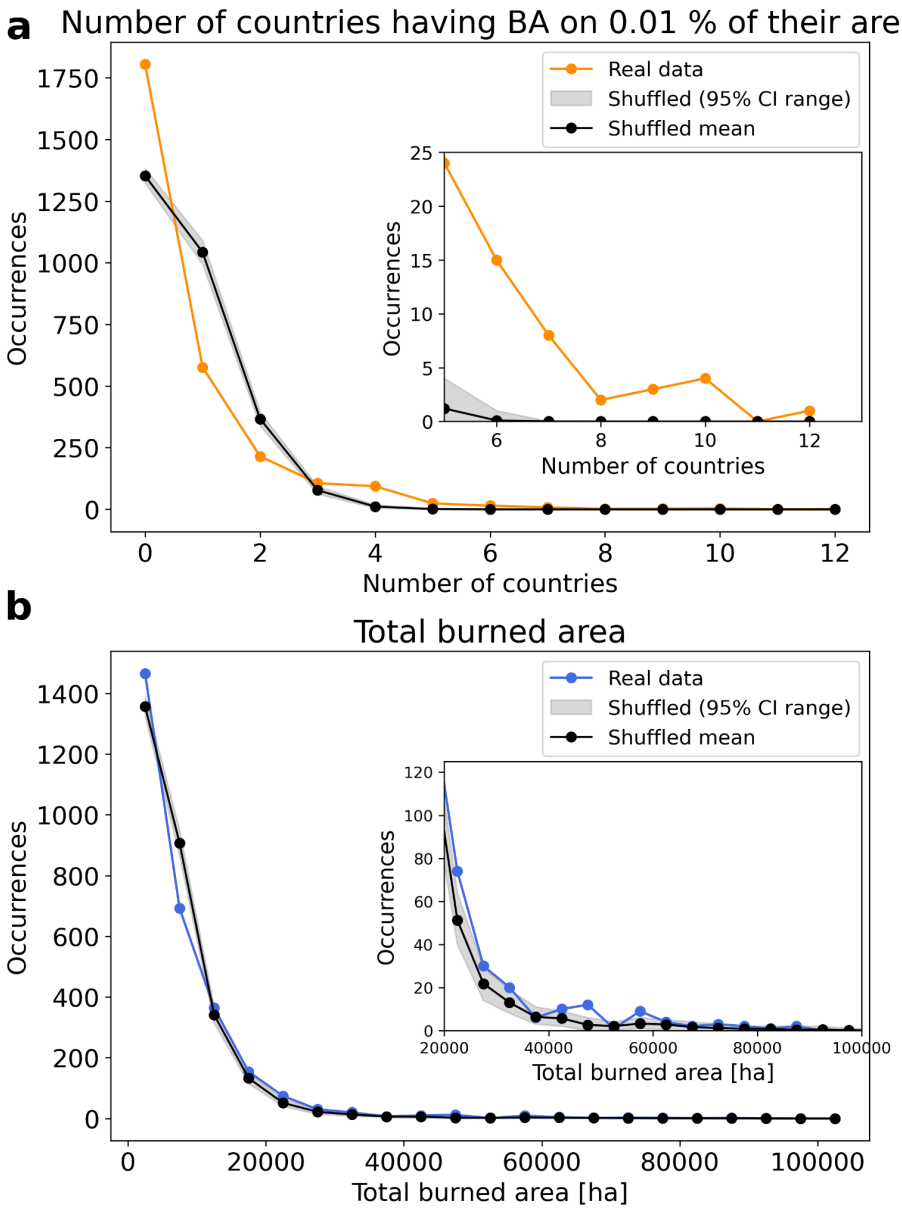

Supplementary Fig. 3. ***Impact of cross-country burned area (BA) correlations on spatially compounding BA metrics over Europe.*** ***a*** *Distribution of the number of countries during the fire season experiencing 0.01% of their area burned on the same day in observations (orange) and in shuffled data where cross-country BA correlations are removed (black; see Methods). For the shuffled data, dots and shading indicate, respectively, the mean and the 95% confidence interval from 1,000 random spatial shuffles. The inset highlights the upper tail.* ***b*** *Same as panel a but for the effect of the cross-country BA correlations on the European-total daily burned area.*

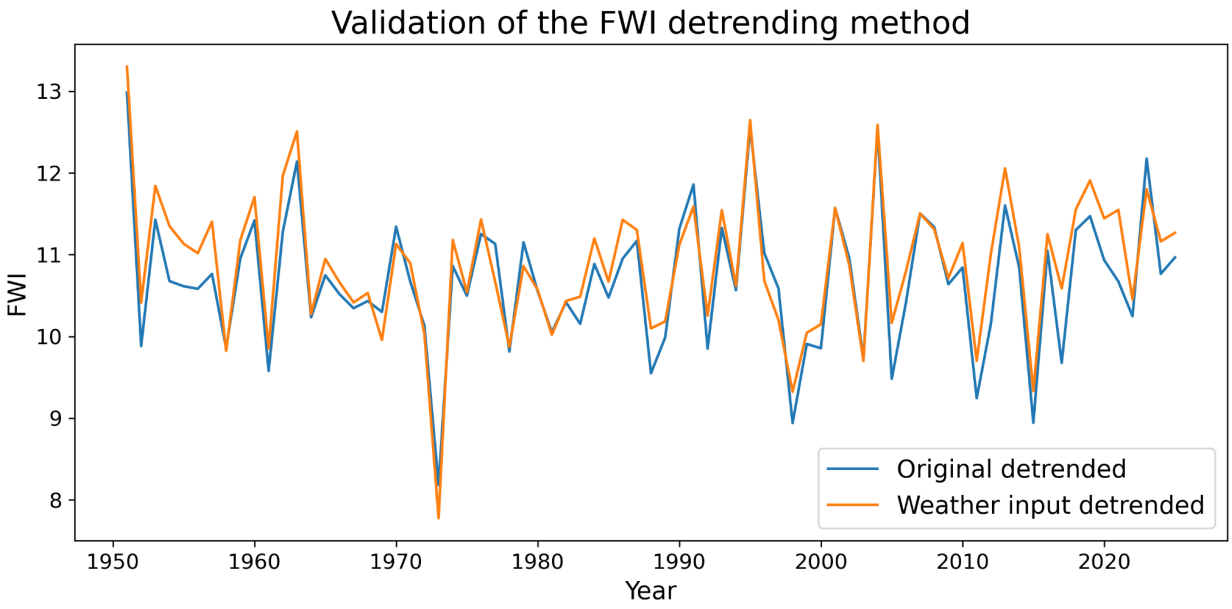

Supplementary Fig. 4. ***Validation of the FWI detrending method.*** *Comparison between the fire season average FWI time series over Europe obtained (i) after detrending the original FWI field (blue) and (ii) from computing FWI using detrended meteorological drivers (temperature, precipitation, relative humidity, and wind speed; orange) (see Methods).*

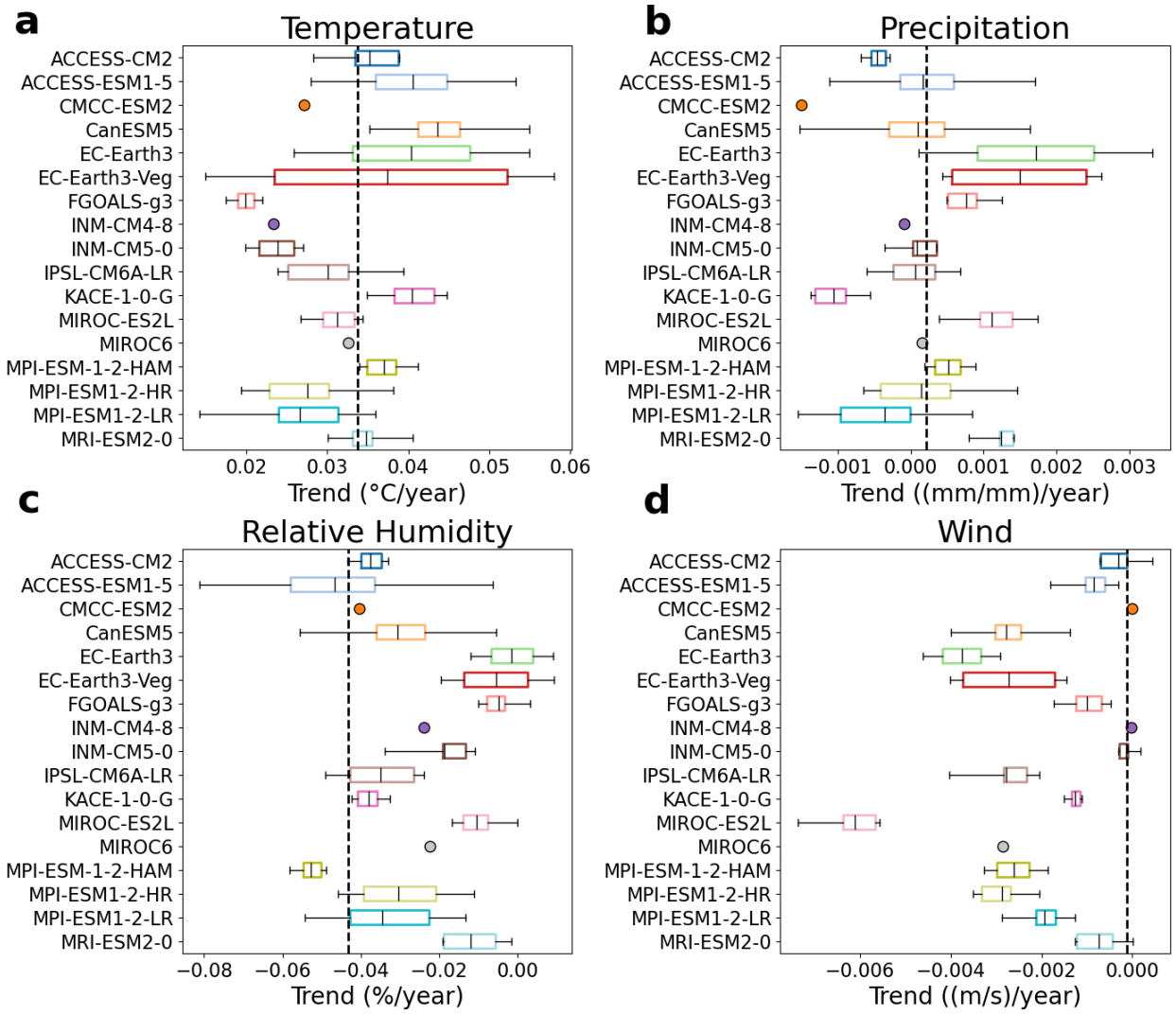

49

50 *Supplementary Fig. 5.* ***Comparison of long-term meteorological drivers trends***
51 ***between ERA5 and CMIP6 models.*** *Linear trends in scaling factors of meteorological*
52 *drivers for 1960-2015 (see Methods), averaged over Europe during the fire season (May-*
53 *October) for* ***a*** *Daily maximum temperature,* ***b*** *Precipitation,* ***c*** *Daily minimum relative*
54 *humidity, and* ***d*** *Wind speed. Each boxplot represents an individual CMIP6 model: the*
55 *vertical line within each box shows the mean of the trend across ensemble members, the*
56 *box shows the interquartile range, and the whiskers illustrate the full range across*
57 *ensemble members. Models with a single ensemble member are shown as dots. The*
58 *vertical black dashed line marks the corresponding trend from ERA5.*

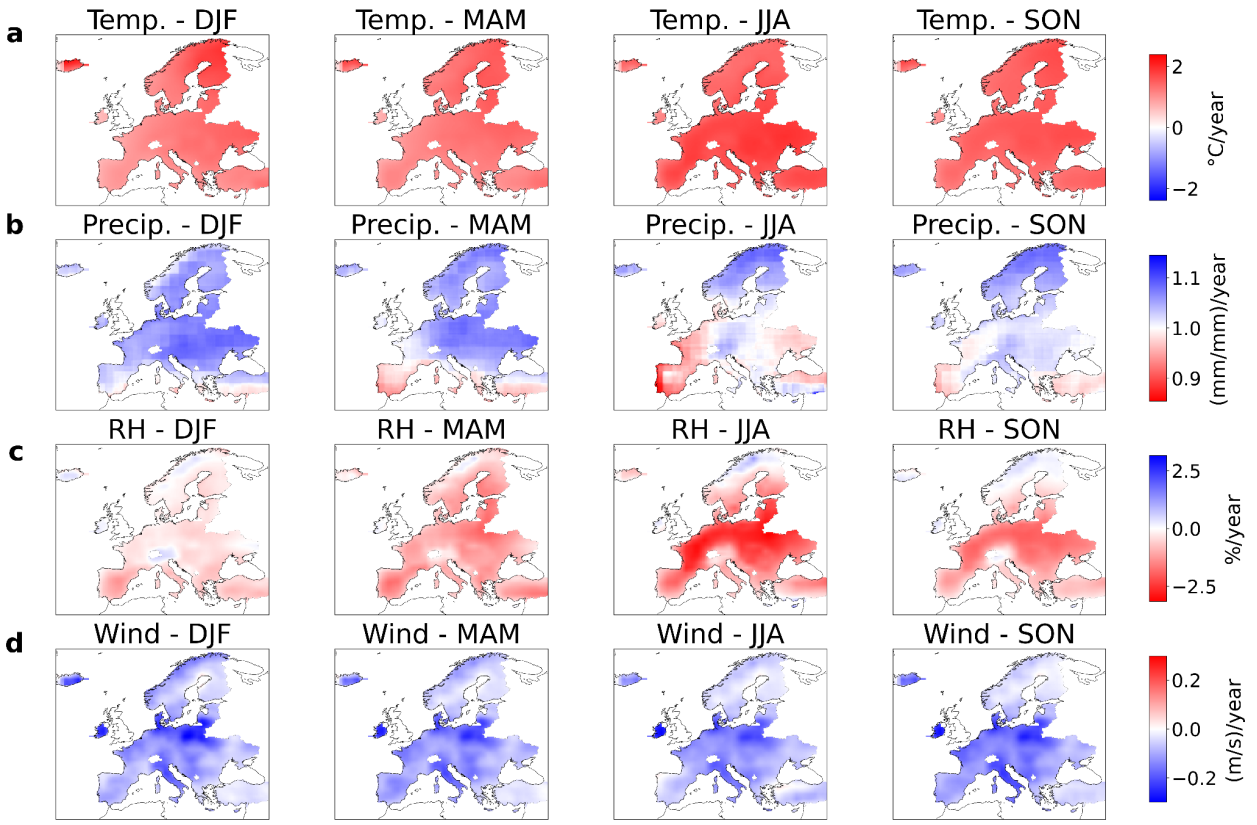

Supplementary Fig. 6. ***Seasonal climate trends in fire weather drivers across Europe.*** *Linear trends from 1994 to 2024 in scaling factors of meteorological variables, derived from CMIP6 climate models. Linear trends for* ***a*** *daily maximum temperature,* ***b*** *precipitation,* ***c*** *daily minimum relative humidity, and* ***d*** *wind speed; each displayed across the four seasons: December to February (DJF), March to May (MAM), June to August (JJA) and September to November (SON). (These scaling factors were also derived using 1950-1980 as a reference period).*

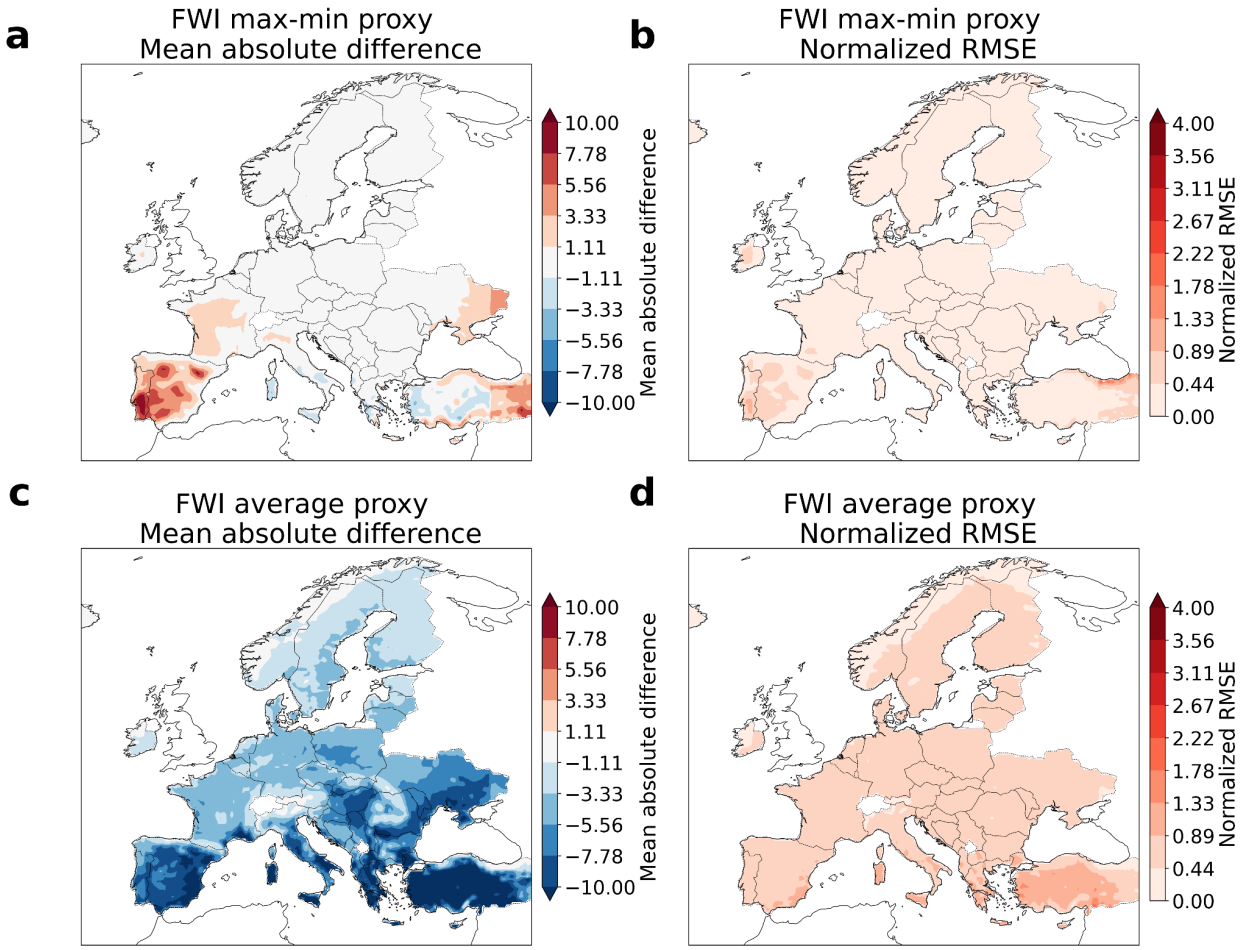

Supplementary Fig. 7. ***Performance of two daily FWI proxies relative to the standard local noon-based FWI over 1950–2024 during the fire season.*** *Mean absolute difference (**a**) and normalized RMSE (**b**) between the standard FWI computed at local noon (the local noon time was derived based on the longitude of each grid point) and FWI based on the max–min proxy employed for analyses in this paper, which uses daily maximum temperature, daily precipitation sum, minimum relative humidity, and daily mean wind speed.* ***c,d*** *The same as panel (a,b), but comparing the standard FWI against the FWI based on the daily-average proxy, which is based on daily mean temperature, daily precipitation sum, daily mean relative humidity, and daily mean wind speed.*

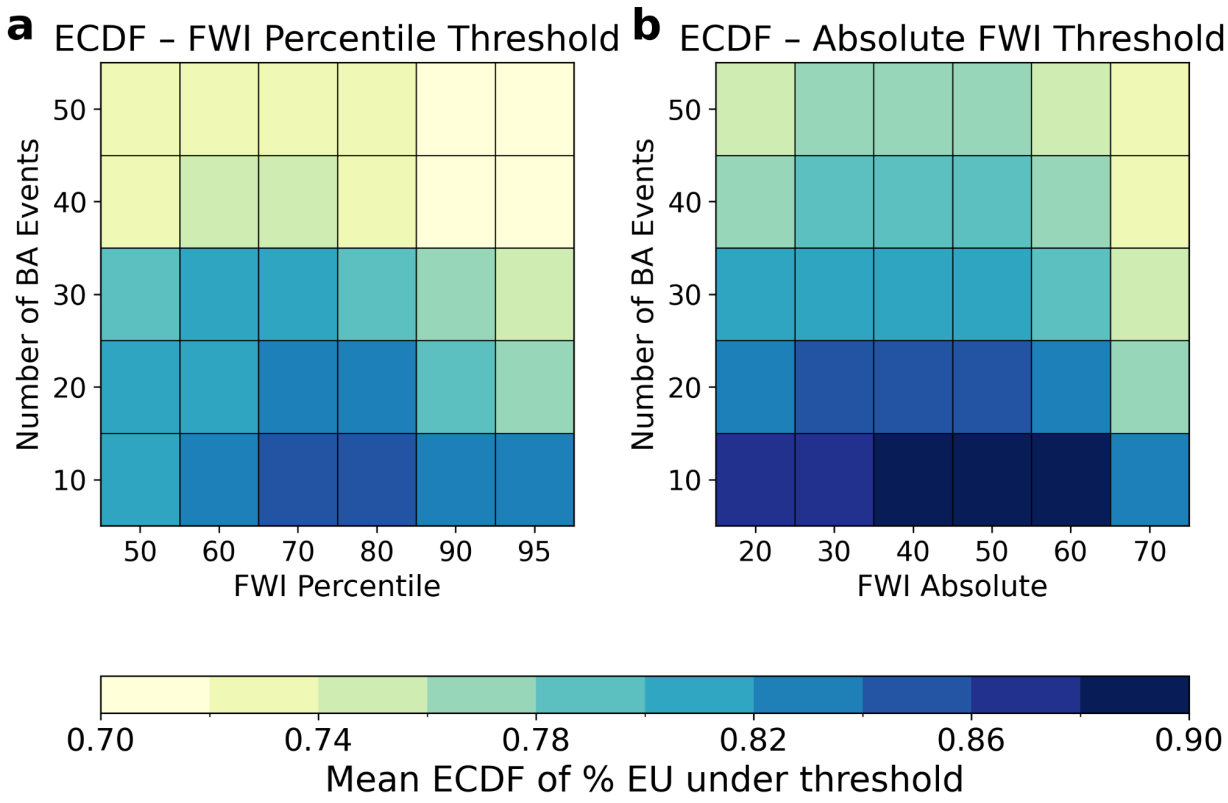

77

78 *Supplementary Fig. 8.* ***Definition of extreme FWI threshold a*** *Average empirical*
79 *cumulative distribution function (ECDF) value of the percentage of European land*
80 *exceeding different percentile-based FWI thresholds (x-axis) averaged over the largest N*
81 *(N = 10, 20, 30, 40, 50) European-total BA daily events (y-axis), during the fire season*
82 *2001-2015. Darker colors indicate higher average ECDF values, reflecting stronger*
83 *correspondence between high FWI conditions and extreme BA events.* ***b*** *As panel a, but*
84 *using different absolute-based FWI thresholds, which are shown on the x-axis.*